eLIFE
elifesciences.org

RESEARCH ARTICLE

Figures and figure supplements

Non-canonical Wnt signalling modulates the endothelial shear stress flow sensor in vascular remodelling

Claudio A Franco *et al*

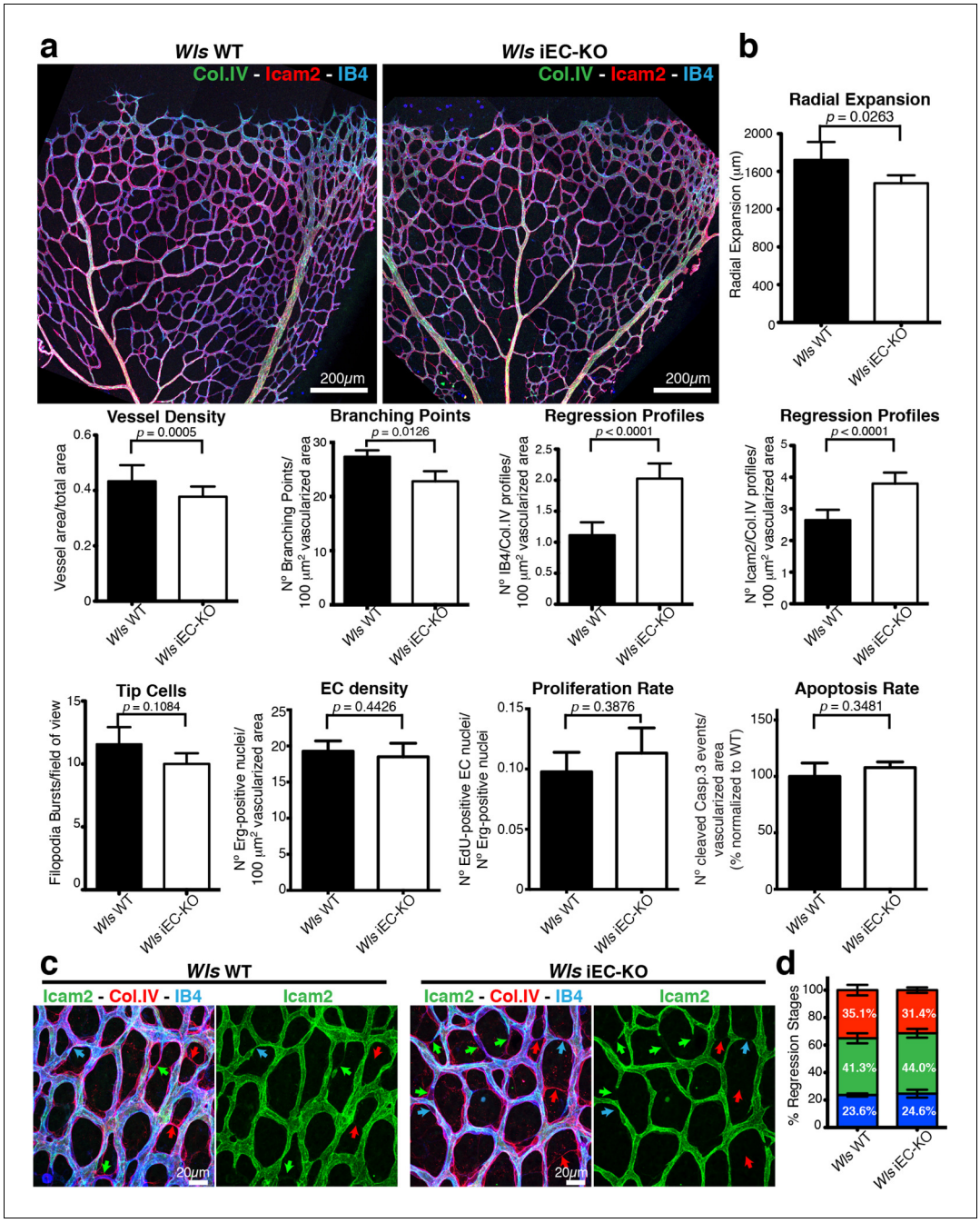

Figure 1. EC-derived Wnt ligands protect against vessel regression. (**a**) Overview of retinal vascular plexus of P6 control and *Wls* iEC-KO mice, labeled for lumen (ICAM2), ECs (IB4) and ECM (Col.IV). (**b**) Quantification of vascular parameters demonstrating that increased vessel regression is a main feature of *Wls* iEC-KO in P6 retinas. IB4/Col. IV regression profiles correspond to the number Col.IV-positive segments negative for IB4 staining. ICAM2/Col.IV regression profiles correspond to number of Col.IV-positive vessel segments partially or totally negative for ICAM2 staining. p values from unpaired, two-tailed t-test. Mean +/-SEM; N = 6 mice; 3 litters. (**c**) High magnification images of the vascular plexus of control and *Wls* iEC-KO mice marked for each stage of vessel regression (stenosis, blue arrows; retraction, green arrow; resolution, red arrows). (**d**) Quantification of the each specific vessel regression stage in *Wls* iEC-KO and *Wls* WT P6 retinas (stenosis, blue bars; retraction, green bars; resolution, red bars). Two-way ANOVA with Sidak multiple comparisons test. Mean +/-SEM; N = 5 mice; 3 litters; N = 288 and N = 398 regression events for *Wls* WT and *Wls* iEC-KO mice, respectively.

DOI: 10.7554/eLife.07727.004

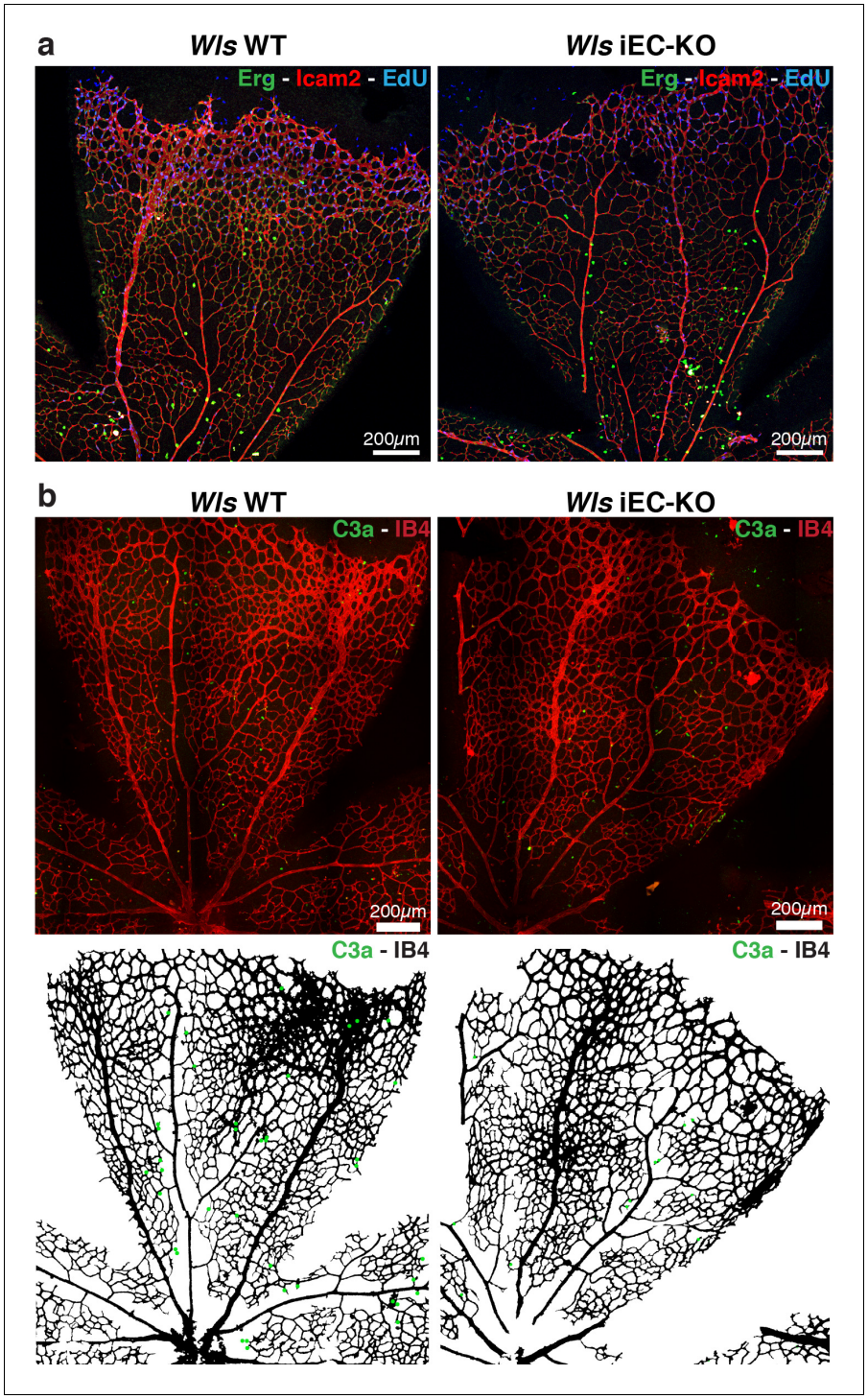

Figure 1—figure supplement 1. *Wls* iEC-KO mice show normal proliferation and apoptosis rates.
(**a**) Representative confocal images of proliferation profile in *Wls* iEC-KO and *Wls* WT P6 mouse retinas labeled with ICAM2 (red), endothelial cell nuclei (Erg, green) and EdU (blue). (b) Representative segmentation of confocal images stained for active caspase-3 and blood vessels (IB4) showing distribution of endothelial cells positive for active caspase-3 (green dots) in *Wls* iEC-KO and *Wls* WT P6 mouse retinas.
DOI: 10.7554/eLife.07727.005

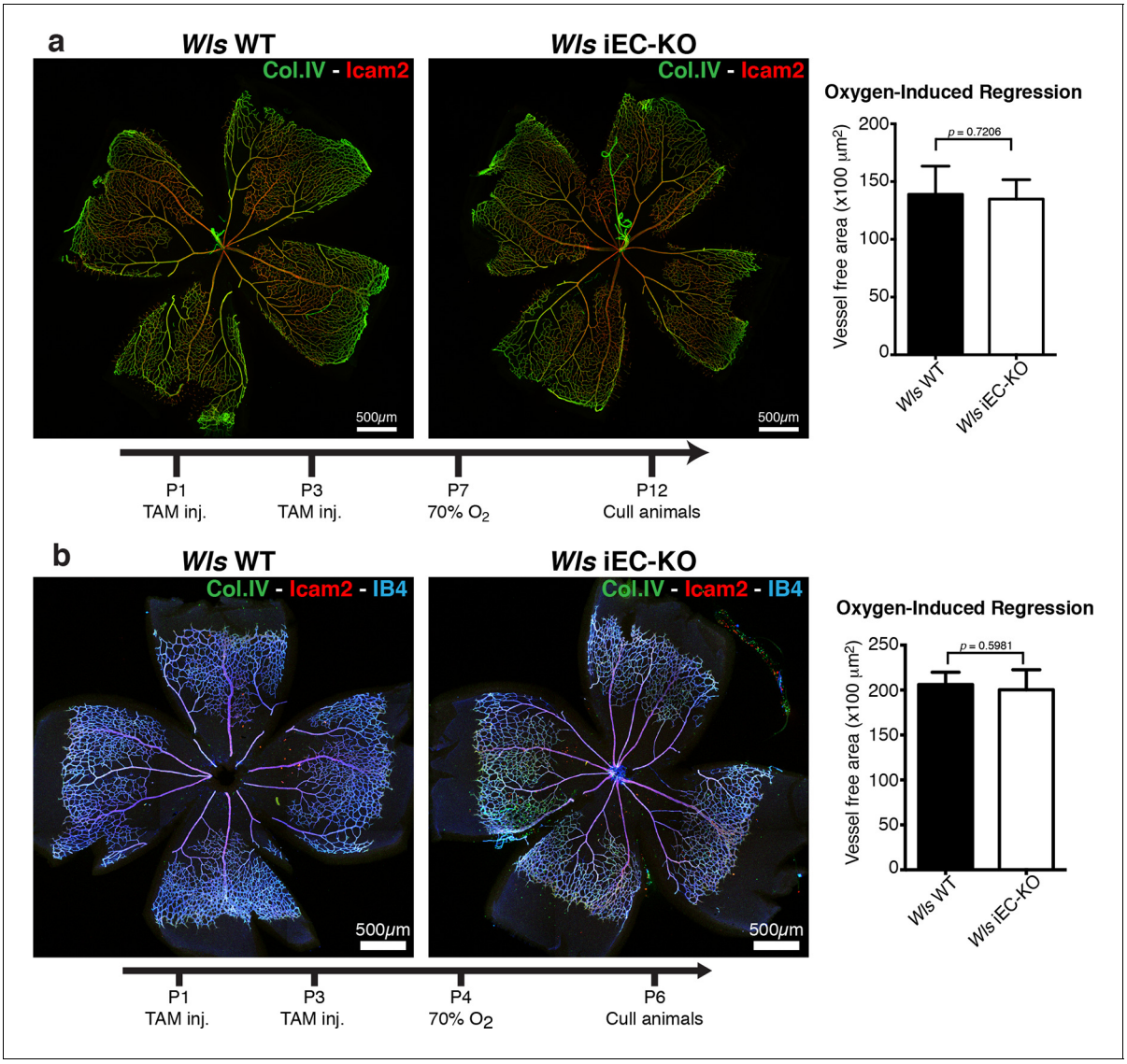

Figure 2. Oxygen-induced vessel regression is not enhanced in *Wls* iEC-KO mice. (**a**) Representative confocal images of *Wls* iEC-KO and *Wls* WT P12 mouse retinas under 70% oxygen concentration from P7 until P12, and labeled for vessel lumen (Icam2, red) and extracellular matrix (Col.IV, green). Quantification shows no significant difference in area of vessel obliteration between *Wls* iEC-KO and *Wls* WT mouse. p values from unpaired, two-tailed t-test. Mean +/-SEM; N = 6 mice; 2 litters. (**b**) Representative confocal images of *Wls* iEC-KO and *Wls* WT P16 mouse retinas under 70% oxygen concentration from P4 until P6, and labeled with vessel lumen (Icam2, red), endothelial cells (IB4, blue) and extracellular matrix (Col.IV, green). Quantification shows no significant difference in area of vessel obliteration between *Wls* iEC-KO and *Wls* WT mouse. p values from unpaired, two-tailed t-test. Mean +/-SEM; N = 6 mice; 3 litters.

DOI: 10.7554/eLife.07727.006

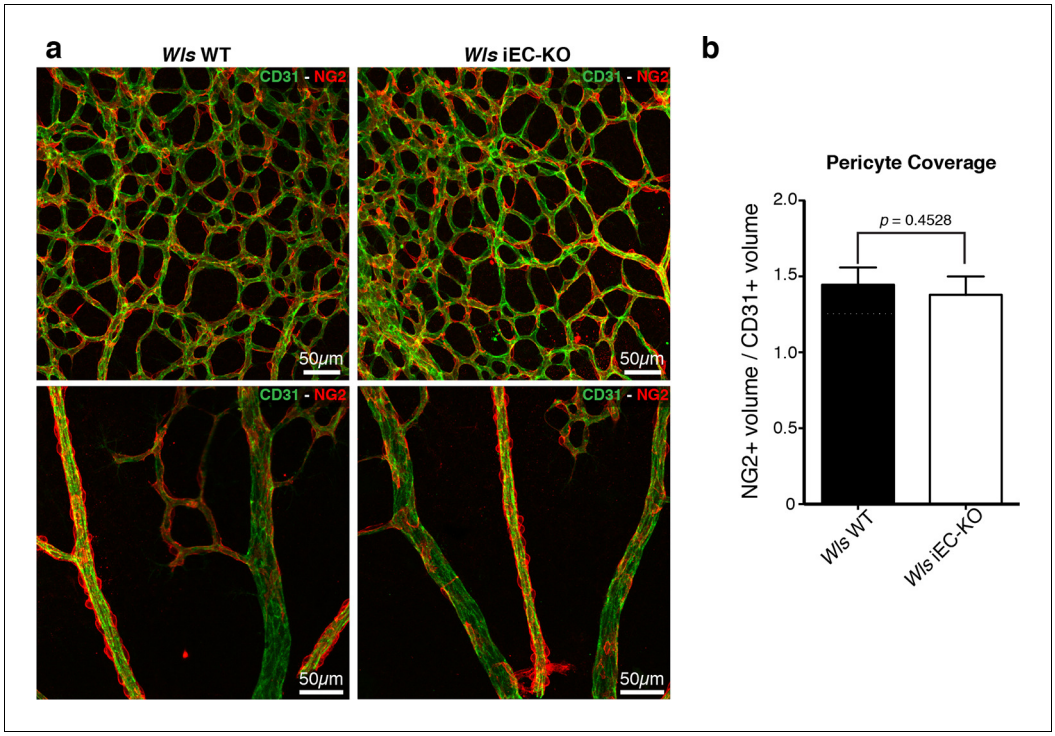

Figure 3. Normal pericytic coverage in *Wls* iEC-KO. (**a**) Overview of retinal vascular plexus of P6 control and *Wls* iEC-KO mice, labeled for endothelial cells (CD31), and pericytes (Ng2), in capillary plexus (top panels) and main vessels (bottom panels). (**b**) Quantification of pericyte coverage of retinal blood vessels, showing no significant change between control and *Wls* iEC-KO in P6 retinas. p values from unpaired, two-tailed t-test. Mean +/-SEM; N = 4 mice; 2 litters.

DOI: 10.7554/eLife.07727.007

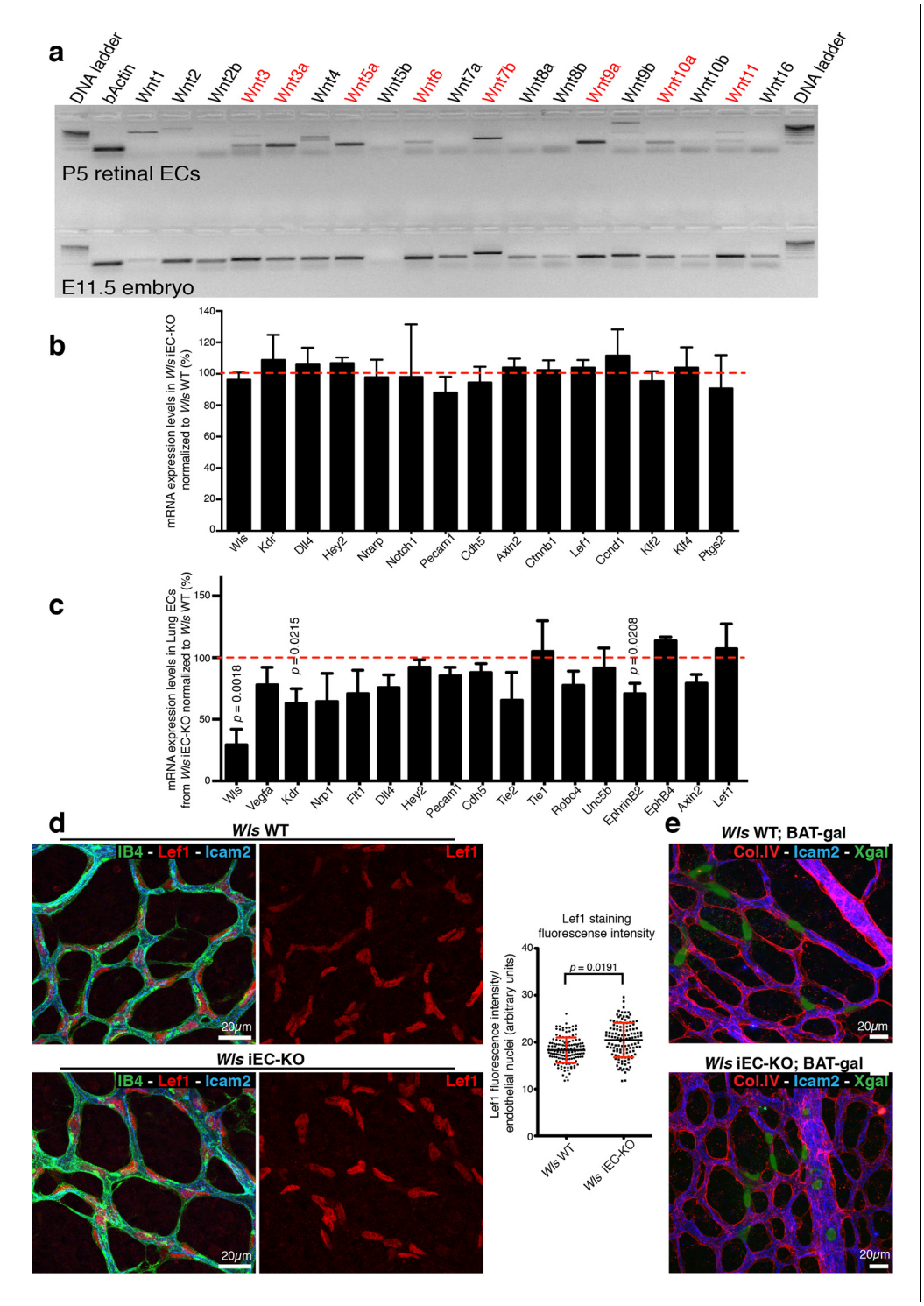

Figure 4. *Wls* iEC-KO show no significant defects in canonical Wnt signalling. (**a**) RT-PCR for all known mouse Wnt ligands using mRNA extracts from isolated retinal endothelial cells of P7 wild-type retinas (red text represents positive bands). (**b**) Semi-quantitative real-time analysis of mRNA expression levels of different genes in P6 *Wls* iEC-KO retinas normalized to *Wls* WT retinas from whole retina extracts. p values from unpaired, two-tailed t-test. Mean +/- SD; N = 4 mice; 2 litters. (**c**) Semi-quantitative real-time analysis of mRNA expression levels of different genes in P6 *Wls* iEC-KO normalized to *Wls* WT from isolated lung endothelial cells. p values from unpaired, two-tailed t-test. Mean +/-SEM; N = 3 mice; 2 litters. (**d**) Lef1 immunostaining and quantification of fluorescence intensity (graph right) in endothelial cells (IB4) from *Wls* iEC-KO and *Wls* WT retinas. p values from unpaired, two-

Figure 4 continued on next page

Figure 4 continued

tailed t-test. Mean +/- SEM; N = 234 *Wls* WT cells and N = 128 *Wls* iEC-KO cells; 4 mice. (**e**) X-gal staining, indicative of canonical Wnt signalling activation, in *Wls* iEC-KO; BAT-gal and *Wls* WT; BAT-gal retinas. No correlation was found with X-gal positive cells and regression profiles (visualized by ECM (Col.IV) and lumen (Icam2) stainings).

DOI: 10.7554/eLife.07727.008

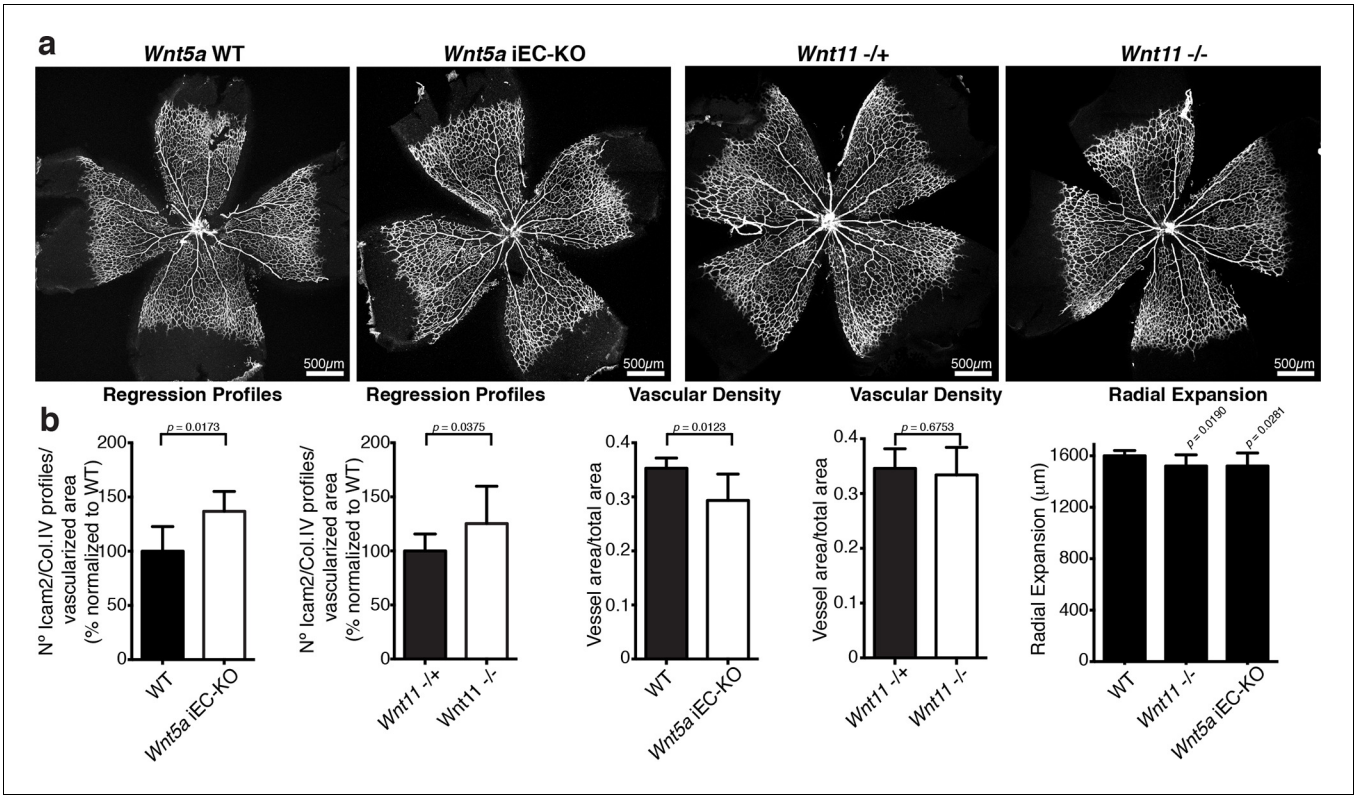

Figure 5. Characterization of vascular parameters in *Wnt5a* iEC-KO and *Wnt11* KO retinas. (**a**) Overview of retinal vascular plexus of P6 *Wnt5a* iEC-KO, *Wnt11* KO, and corresponding control mice, labeled with ECM (Col.IV, grey). (**b**) Quantification of different vascular parameters in P6 retinas on the different mouse strains. p values from unpaired, two-tailed t-test. Mean +/-SEM; N = 5 mice; 3 litters.

DOI: 10.7554/eLife.07727.009

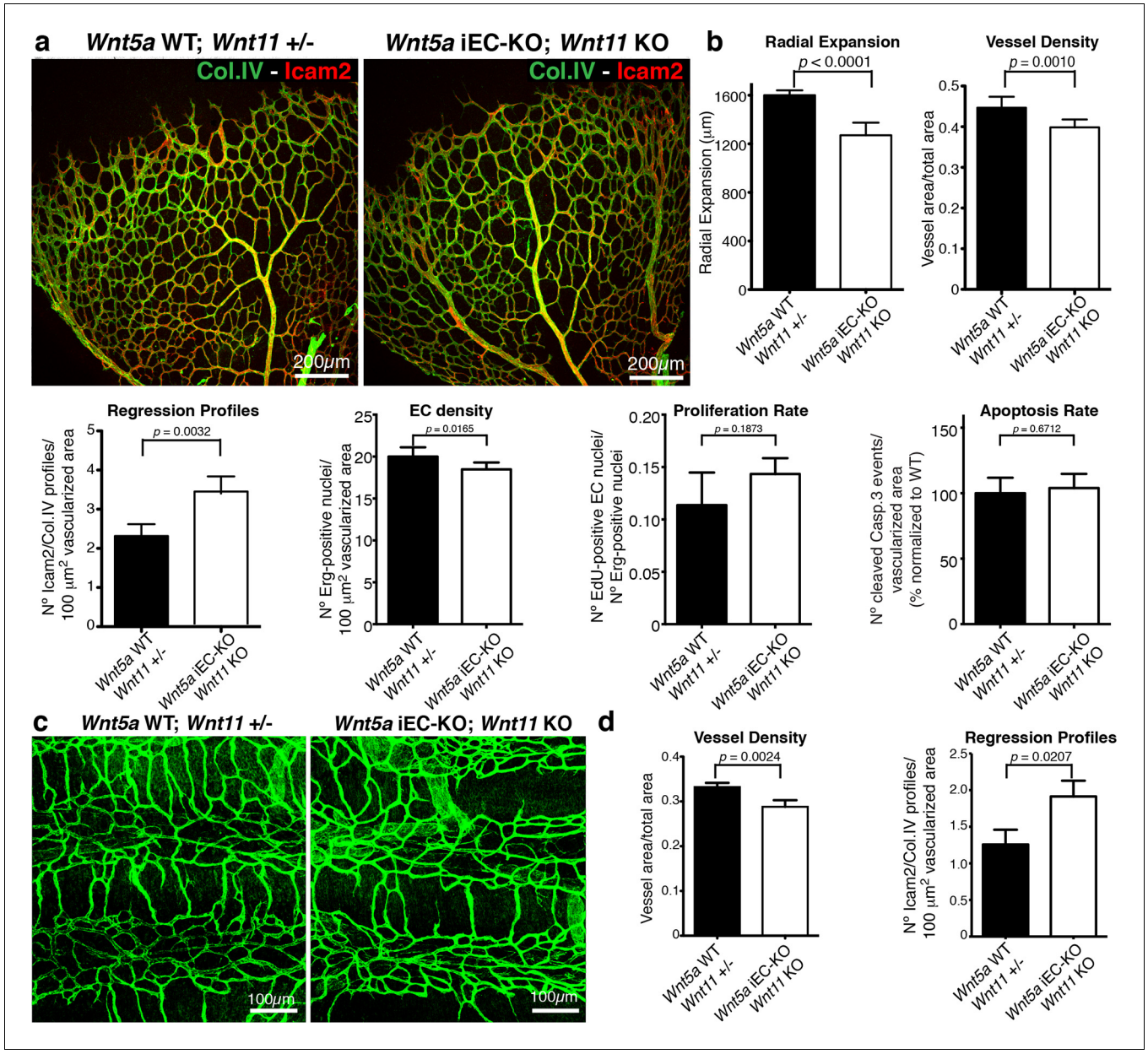

Figure 6. Non-canonical Wnt signalling regulates vessel regression. (**a**) Overview of retinal vascular plexus of control and compound *Wnt5a* iEC-KO; *Wnt11* KO mice, labelled with lumen (Icam2) and ECM (Col.IV) markers. (**b**) Quantification of different vascular parameters showing increased vessel regression in *Wnt5a* iEC-KO; *Wnt11* KO retinas. p values from unpaired, two-tailed t-test. Mean +/-SEM; N = 7 mice; 3 litters. (**c**) Overview of trachea vascular plexus of P6 *Wnt5a* iEC-KO; *Wnt11* KO and control mice labelled for CD31 (green). (**d**) Quantification of vessel density and regression profiles in the trachea of *Wnt5a* iEC-KO; *Wnt 11* KO and WT P6 mice. p values from unpaired, two-tailed t-test. Mean +/-SEM; N = 4 mice; 2 litters.

DOI: 10.7554/eLife.07727.010

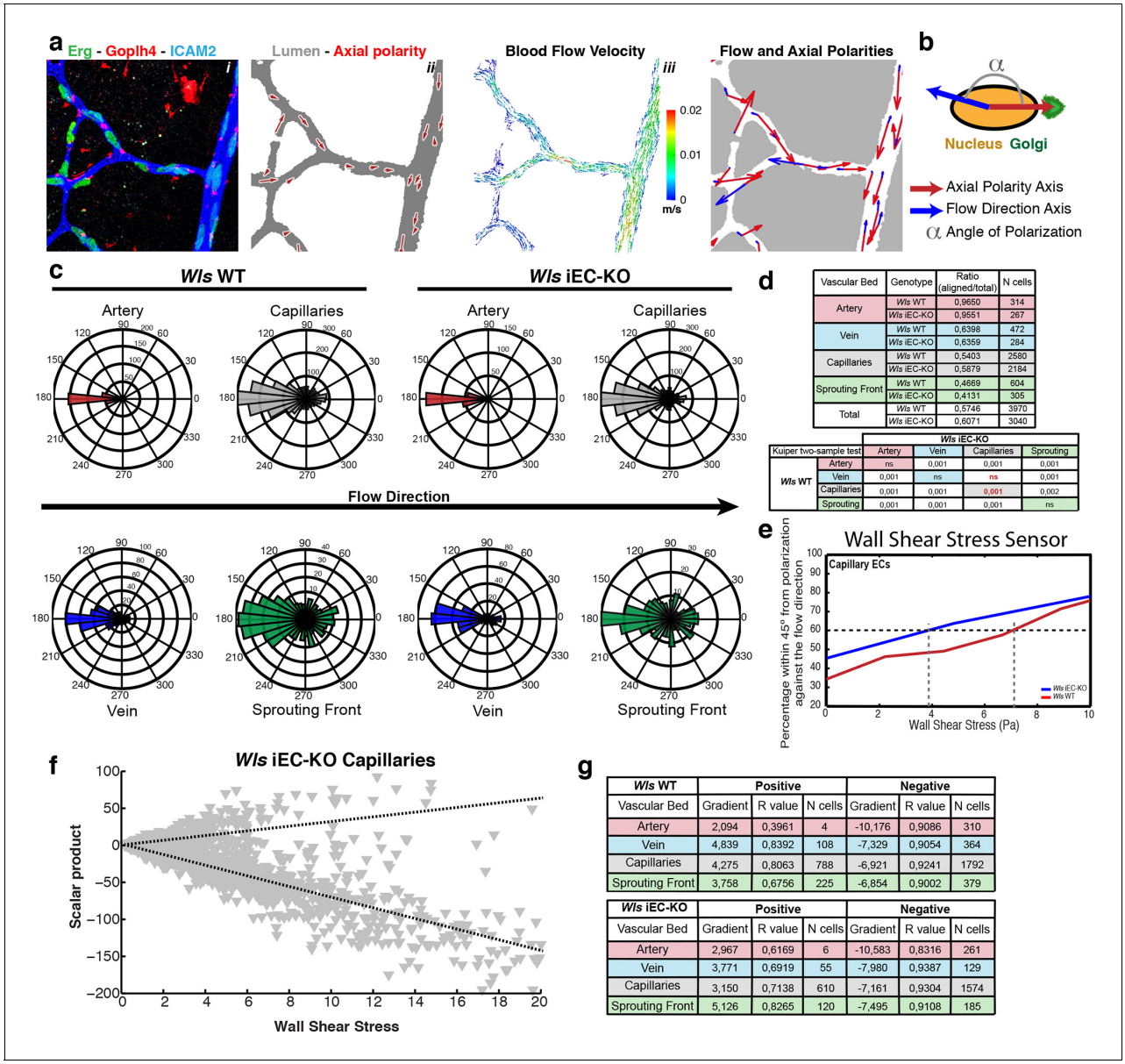

Vascular Bed	Genotype	Ratio (aligned/total)	N cells
Artery	*Wls* WT	0,9650	314
	Wls iEC-KO	0,9551	267
Vein	*Wls* WT	0,6398	472
	Wls iEC-KO	0,6359	284
Capillaries	*Wls* WT	0,5403	2580
	Wls iEC-KO	0,5879	2184
Sprouting Front	*Wls* WT	0,4669	604
	Wls iEC-KO	0,4131	305
Total	*Wls* WT	0,5746	3970
	Wls iEC-KO	0,6071	3040

Kuiper two-sample test		*Wls* iEC-KO			
		Artery	Vein	Capillaries	Sprouting
Wls WT	Artery	ns	0,001	0,001	0,001
	Vein	0,001	ns	ns	0,001
	Capillaries	0,001	0,001	0,001	0,002
	Sprouting	0,001	0,001	0,001	ns

Wls WT	Positive			Negative		
Vascular Bed	Gradient	R value	N cells	Gradient	R value	N cells
Artery	2,094	0,3961	4	-10,176	0,9086	310
Vein	4,839	0,8392	108	-7,329	0,9054	364
Capillaries	4,275	0,8063	788	-6,921	0,9241	1792
Sprouting Front	3,758	0,6756	225	-6,854	0,9002	379

Wls iEC-KO	Positive			Negative		
Vascular Bed	Gradient	R value	N cells	Gradient	R value	N cells
Artery	2,967	0,6169	6	-10,583	0,8316	261
Vein	3,771	0,6919	55	-7,980	0,9387	129
Capillaries	3,150	0,7138	610	-7,161	0,9304	1574
Sprouting Front	5,126	0,8265	120	-7,495	0,9108	185

Figure 7. Endothelial-derived Wnt ligands modulate endothelial polarization in response to wall shear stress. (**a**) Example of axial polarity of an *Wls* iEC-KO P6 retina, labeled for EC nuclei (Erg), lumen (Icam2) and Golgi (Golph4) (i), corresponding image segmentation of the vascular plexus with axial polarity vectors in red (ii), flow pattern simulation of the selected area (iii), and correlation between axial polarity and blood flow direction at the endothelial nuclear position (iv). (**b**) Representation of the principle of angle calculation between axial and flow polarities of endothelial nuclei in (a), highlighting the lumen of blood vessels (grey), and the axial polarity of all ECs (red arrows). (**c**) Analysis of the endothelial axial polarity angle in the main vessels, relative to predicted blood flow direction by the rheology in silico model in *Wls* WT and *Wls* iEC-KO mice (n = 3 retinas). (**d**) Quantitative analysis of the percentage of ECs polarized at 180°(± 45°) degrees compared to the flow direction in the different vascular beds of *Wls* WT and *Wls* iEC-KO mice (n = 3 retinas). (**e**) Correlative analysis of wall shear stress and EC polarization in the capillary vascular bed of *Wls* WT and *Wls* iEC-KO mice. (**f**) Representative graph showing the distribution of scalar products in function to wall shear stress levels for ECs from *Wls* iEC-KO capillaries. Scalar product corresponds to the product between length of the axial polarity vector and the cosine of the angle between the axial polarity vector and the flow direction vector. (**g**) Linear regression analysis of positive (polarized with flow) and negative (polarized against the flow) scalar product points for each endothelial cell nucleus. Gradient, R-value and number of cells analyzed for each vascular bed and genotype are shown. N = 3 retinas.

DOI: 10.7554/eLife.07727.011

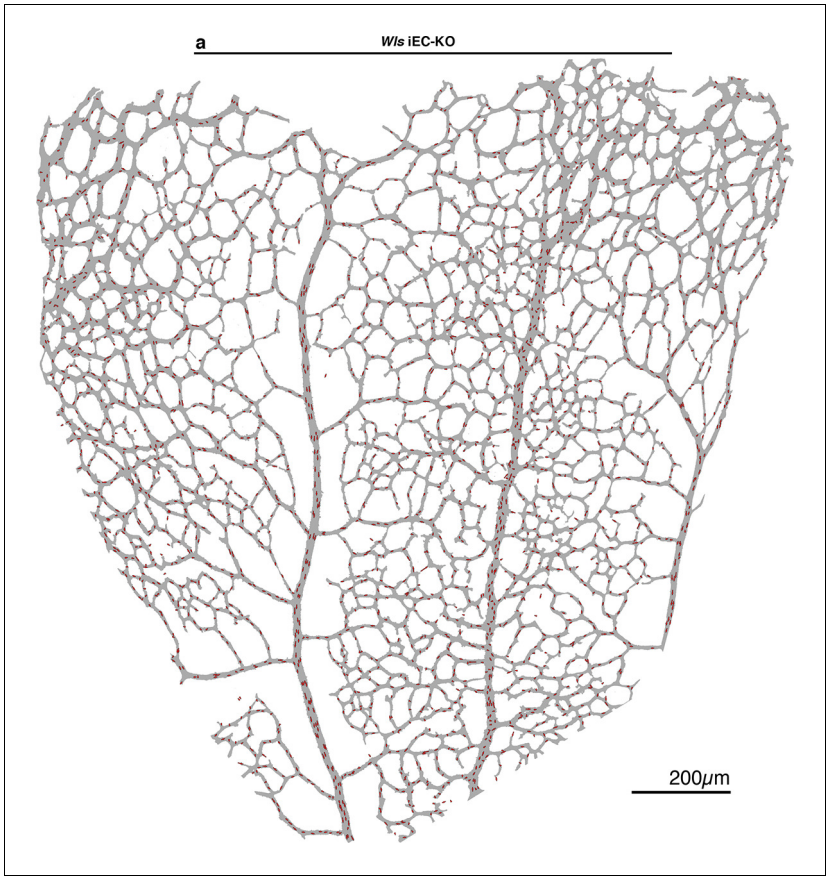

Figure 7—figure supplement 1. Endothelial polarization patterns in *Wls* iEC-KO. (**a**) Image segmentation of the vascular plexus of an *Wls* iEC-KO mouse retina, highlighting the lumen of blood vessels (grey) and the nucleus-to-golgi (axial) polarity of all endothelial cells (red arrows).

DOI: 10.7554/eLife.07727.012

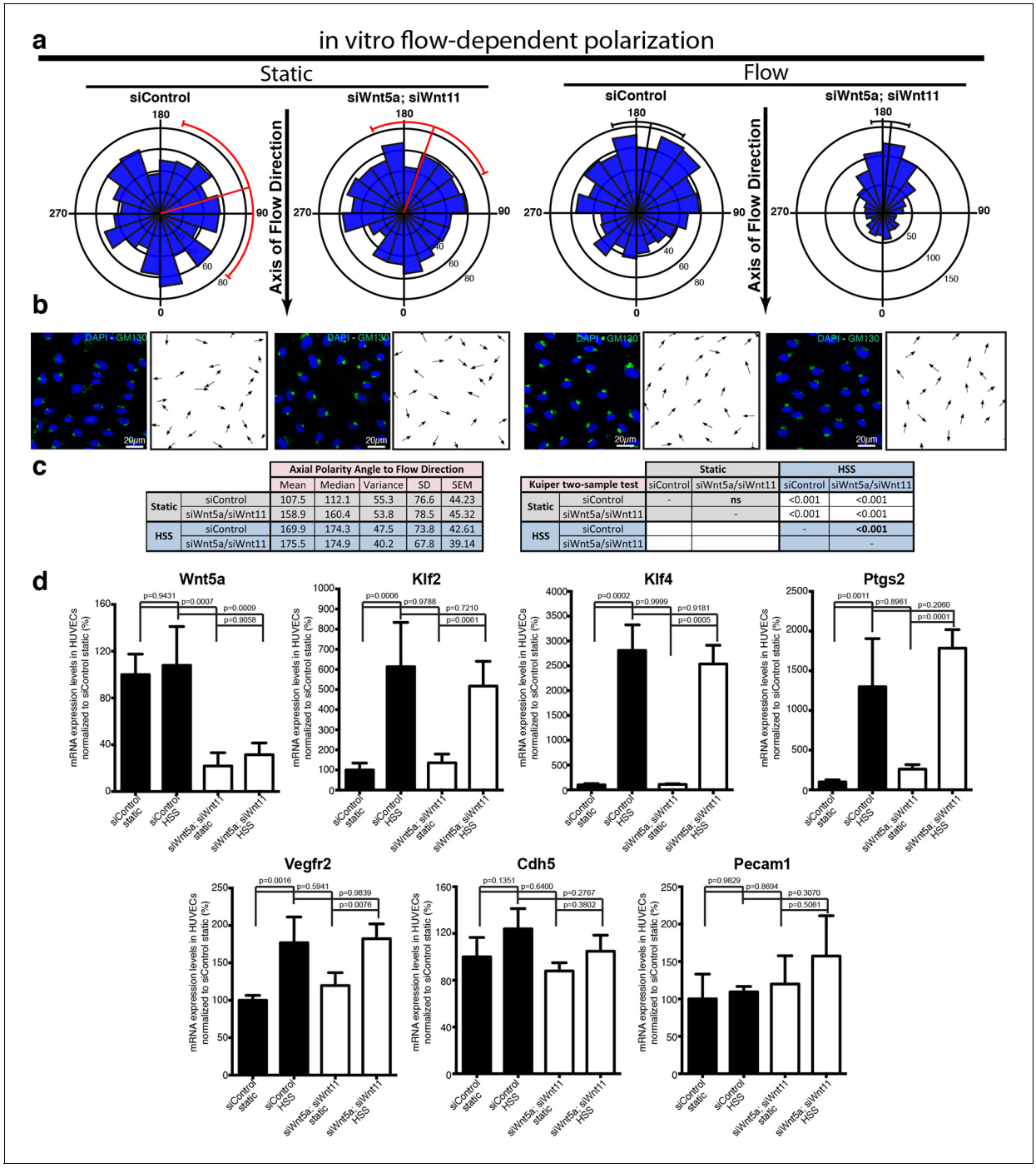

		Axial Polarity Angle to Flow Direction				
		Mean	Median	Variance	SD	SEM
Static	siControl	107.5	112.1	55.3	76.6	44.23
	siWnt5a/siWnt11	158.9	160.4	53.8	78.5	45.32
HSS	siControl	169.9	174.3	47.5	73.8	42.61
	siWnt5a/siWnt11	175.5	174.9	40.2	67.8	39.14

Kuiper two-sample test		Static		HSS	
		siControl	siWnt5a/siWnt11	siControl	siWnt5a/siWnt11
Static	siControl	-	ns	<0.001	<0.001
	siWnt5a/siWnt11		-	<0.001	<0.001
HSS	siControl			-	**<0.001**
	siWnt5a/siWnt11				-

Figure 8. Non-canonical Wnt signalling modulates flow-induced polarity but not flow-induced transcriptional gene expression response. (**a**) Rose-plot representation of axial polarity of ECs treated with Control or *Wnt5a* and *Wnt11* specific siRNAs in static conditions or in response to 2 Pa flow in a microfluidic device (n = 3 independent experiments). Line running from the center represents the Mean of the dataset. Arcs extending to either side represent the 95% confidence limits of the mean (red means not significantly polarised; black means significantly polarised). (**b**) Representative images of endothelial cell polarity in flow chamber stained for nuclei (Dapi, Blue) and Golgi apparatus (GM130, green), and corresponding axial polarity vectors (black arrows). (**c**) Quantitative analysis of EC polarization related to the flow direction in the microfluidic device. p values from non-parametric two-tailed Kuiper's test. (**d**) Semi-quantitative real-time analysis of mRNA expression levels of different genes in Control or *Wnt5a* and *Wnt11* specific siRNAs in static or stimulated with 2 Pa conditions in a microfluidic device. p values from one-way ANOVA with multiple comparisons. Mean +/-SD; N = 3 independent experiments.

DOI: 10.7554/eLife.07727.013

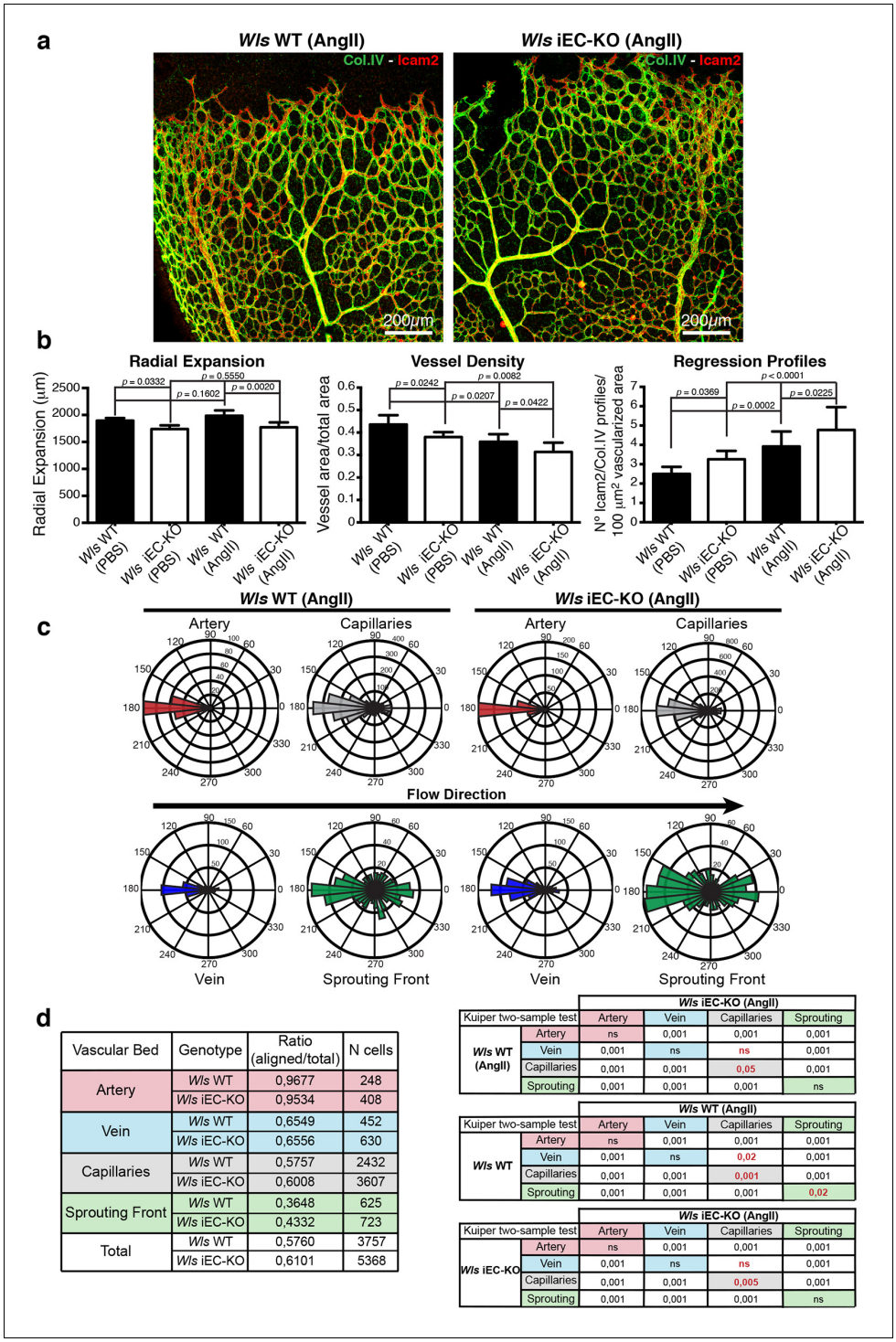

Vascular Bed	Genotype	Ratio (aligned/total)	N cells
Artery	*Wls* WT	0,9677	248
	Wls iEC-KO	0,9534	408
Vein	*Wls* WT	0,6549	452
	Wls iEC-KO	0,6556	630
Capillaries	*Wls* WT	0,5757	2432
	Wls iEC-KO	0,6008	3607
Sprouting Front	*Wls* WT	0,3648	625
	Wls iEC-KO	0,4332	723
Total	*Wls* WT	0,5760	3757
	Wls iEC-KO	0,6101	5368

Kuiper two-sample test		*Wls* iEC-KO (AngII)			
		Artery	Vein	Capillaries	Sprouting
Wls WT (AngII)	Artery	ns	0,001	0,001	0,001
	Vein	0,001	ns	ns	0,001
	Capillaries	0,001	0,001	0,05	0,001
	Sprouting	0,001	0,001	0,001	ns

Kuiper two-sample test		*Wls* WT (AngII)			
		Artery	Vein	Capillaries	Sprouting
Wls WT	Artery	ns	0,001	0,001	0,001
	Vein	0,001	ns	0,02	0,001
	Capillaries	0,001	0,001	0,001	0,001
	Sprouting	0,001	0,001	0,001	0,02

Kuiper two-sample test		*Wls* iEC-KO (AngII)			
		Artery	Vein	Capillaries	Sprouting
Wls iEC-KO	Artery	ns	0,001	0,001	0,001
	Vein	0,001	ns	ns	0,001
	Capillaries	0,001	0,001	0,005	0,001
	Sprouting	0,001	0,001	0,001	ns

Figure 9. Systemic Angiotensin-II treatment accelerates vessel regression independent of Wnt signalling. (**a**) Overview of retinal vascular plexus of P7 control and *Wls* iEC-KO mice treated with angiotensin II, labelled for lumen (Icam2) and ECM (Col.IV). (**b**) Quantification of radial expansion, vessel density and regression profiles in angiotensin II-treated and PBS-treated control retinas. p values from one-way ANOVA with Holm-Sidak's multiple comparison test. Mean +/-SEM; N = 4 mice; 3 litters. (**c**) Analysis of the endothelial axial polarity angle in the main vessels, correlated to predicted blood flow direction by the rheology in silico model in *Wls* WT and *Wls* iEC-KO mice treated with angiotensin II. (**d**) Quantitative analysis of the percentage of ECs polarized at 180°(± 45°) degrees compared to the flow direction in the different vascular beds of *Wls* WT and *Wls* iEC-KO mice with and without angiotensin II treatment (n = 3 retinas).

Figure 9 continued on next page

Figure 9 continued

DOI: 10.7554/eLife.07727.014

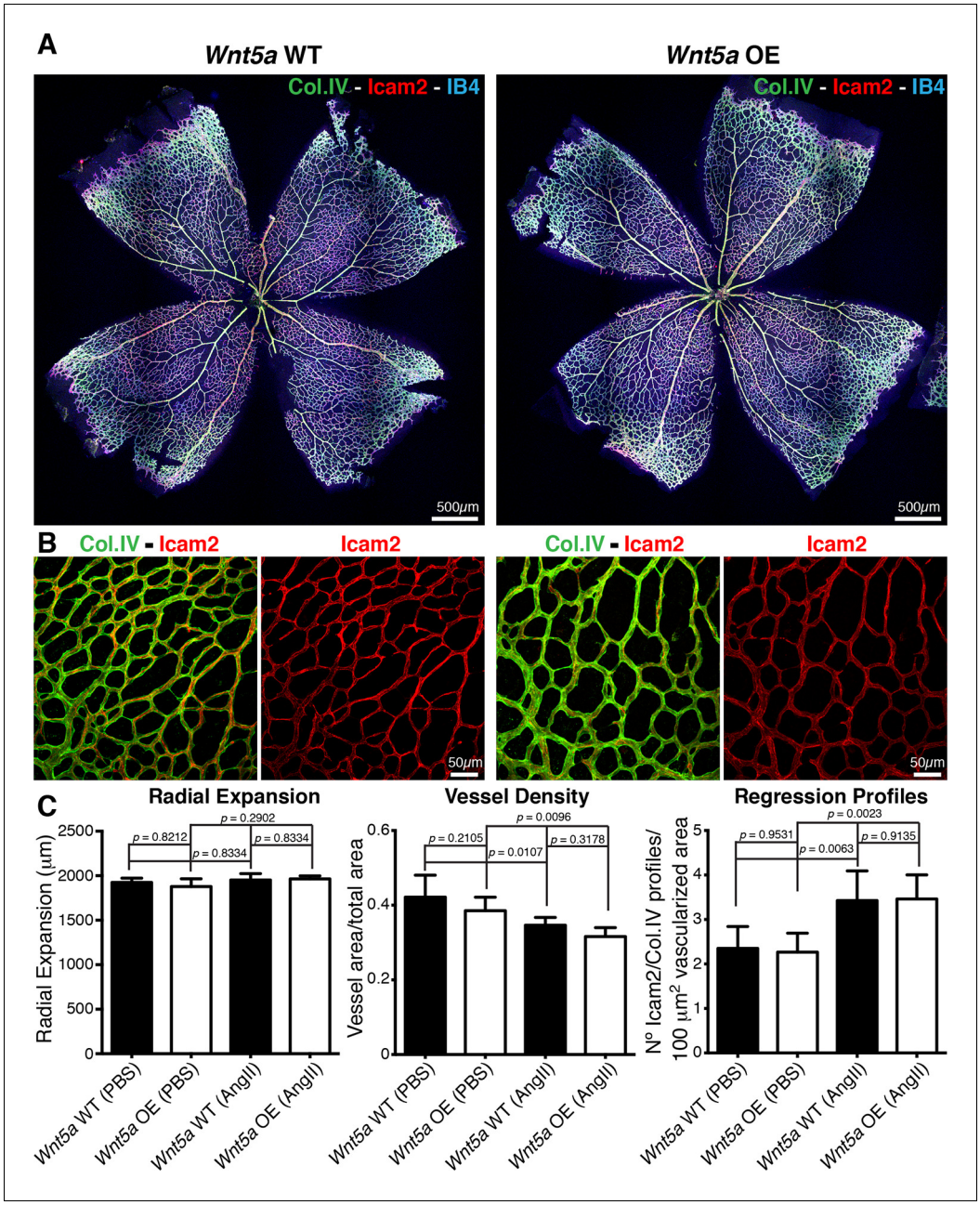

Figure 10. Overexpression of *Wnt5a* in endothelial cells does not inhibit vessel regression. (**a**) Overview of retinal vascular plexus of P6 endothelial-specific *Wnt5a* GOF and corresponding control mice, labeled for ECM (Col.IV, green), blood vessels (IB4, blue) and vascular lumen (Icam2, red). (**b**) Higher magnification of retinal vascular plexus of P6 endothelial-specific *Wnt5a* GOF and corresponding control mice, labeled for ECM (Col.IV, green), blood vessels (IB4, blue) and vascular lumen (Icam2, red). (**c**) Quantification of vascular parameters showing no significant differences between *Wnt5a* GOF and corresponding control retinas, with indicated treatments. p values from one-way ANOVA with Holm-Sidak's multiple comparison test. Mean +/-SEM; N = 4 mice; 2 litters.

DOI: 10.7554/eLife.07727.015

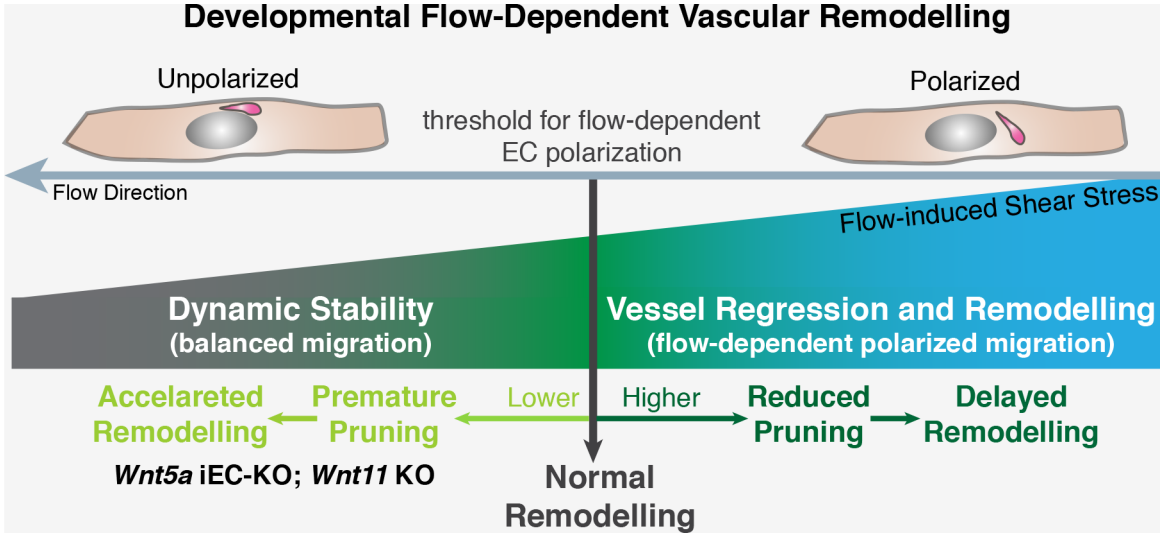

Figure 11. Working model for non-canonical Wnt signalling regulation of flow-induced remodeling. Initiation of the vascular remodeling program is dependent on the level of wall shear stress (threshold) to which ECs robustly polarize against the flow direction. Below the threshold, ECs movements in the immature plexus are balanced by countermovements of adjacent ECs maintaining vessel connections, in a state of dynamic stability. When exposed to shear stress levels above the response threshold, ECs react by polarizing and migrating against the flow direction, triggering vessel regression and vessel remodeling. Signaling pathways influencing the threshold for flow-dependent EC polarization can delay remodeling (raising the threshold) or induce premature remodeling (lowering the threshold), as in the case of deficient non-canonical Wnt signaling.

DOI: 10.7554/eLife.07727.016